Viscous propulsion of a two-dimensional Marangoni boat driven by reaction and diffusion of insoluble surfactant

Darren Crowdy *

Department of Mathematics, Imperial College London, 180 Queen's Gate, London SW7 2AZ, United Kingdom

(Received 22 November 2020; accepted 17 May 2021; published 17 June 2021)

An analytical solution is derived for the flow generated by a self-propelling two-dimensional Marangoni boat driven by reactive insoluble surfactant on a deep layer of fluid of viscosity μ at zero Reynolds number, capillary number, and surface Péclet number. In the model, surfactant emitted from the edges of the boat causes a surface tension disparity across the boat. Once emitted, the surfactant diffuses along the interface and sublimates to the upper gas phase. A linear equation of state relates the surface tension to the surfactant concentration. The propulsion speed of the boat is shown to be $U_0 = \Delta\sigma(2\pi\mu)^{-1}e^{\sqrt{\mathrm{Da}}}K_0(\sqrt{\mathrm{Da}})$ where Da is a Damköhler number measuring the reaction rate of the surfactant to its surface diffusion, $\Delta\sigma$ is the surface tension disparity between the front and rear of the boat, and K_0 is the order-zero modified Bessel function. Explicit expressions for the streamfunction associated with the Stokes flow beneath the boat are found facilitating ready examination of the Marangoni-induced streamlines. An integral formula, derived using the reciprocal theorem, is also given for the propulsion speed of the boat in response to a more general Marangoni stress distribution.

DOI: 10.1103/PhysRevFluids.6.064003

I. INTRODUCTION

The study of self-propelled objects on free surfaces is of extensive current interest [1–3]. One mechanism by which self-propulsion is achieved is by the setting up of a Marangoni stress on an interface: the moving objects are then variously known as "Marangoni boats," or "surfers" [4,5]. The strategic release of surfactants can provoke a surface tension gradient, and a concomitant Marangoni stress, that can lead to locomotion. This phenomenon is familiar in natural biological settings [6] and has also been exploited in synthetic situations [2,3]. External stimuli can also be used to alter the local surface tension to manipulate particles on free surfaces [7–9]. The physics can be complex: surfactants, possibly of multiple species, can diffuse along the surface, or into the bulk fluid, sublimate into an ambient gas phase, or be convected by fluid motions, thereby setting up a surface tension gradient resulting in a Marangoni stress at the interface.

The complexity of the interacting processes calls for theoretical investigation and models of these effects are naturally of interest. In the study of camphor boats [3,10,11]—a type of Marangoni boat whose motion is typically caused by a camphor particle at the rear of the boat that lowers the effective surface tension there—equations of motion are usually written down based on Newton's second law coupled with a reaction-diffusion equation for the surfactant concentration which feeds back to alter the surface tension force appearing in the force imbalance causing motion of the boat [12]. As observed in a recent review [3], few of these models properly account for the surface Marangoni stresses which cause flow in the bulk fluid which then provides a source of additional

*d.crowdy@imperial.ac.uk

forces on the boats. These often neglected Marangoni effects can be important and there is an ongoing effort to understand and model them [11,13,14]. A recent numerical and experimental study [15] has examined Marangoni surfers driven by soluble surfactants and having various shape profiles and in fluid baths of various depths. The flow patterns are visualized over a range of Reynolds numbers and Péclet numbers. An interesting feature is that a forward, backward, or an arrested motion of the surfers can be observed depending on the degree of confinement, a phenomenon that had been observed earlier in theoretical investigations [16].

There is a growing number of theoretical studies of Marangoni propulsion. Under the assumption of zero Reynolds, capillary, and surface Péclet numbers Lauga and Davis [21] found an analytical expression for the Marangoni-induced net speed of propulsion of a floating circular disk as a function of an imposed surfactant distribution at the contact line. This propulsion speed was compared to that obtained by ignoring details of the Marangoni-induced flow altogether and estimating the boat speed instead using a balance of forces between surface tension and the viscous drag on a forced particle; the two speeds, while of the same order of magnitude, are quite different underlining the importance of properly resolving the Marangoni effects. Under the same assumptions on the Reynolds, capillary, and surface Péclet numbers Masoud and Stone [17] used the reciprocal theorem for Stokes flow to calculate the propulsion speed of active oblate and prolate spheroids suspended at interfaces. And motivated by the observation of collective "uniform flow" states of multiple boats interacting on a free surface [18,19] a recent study [20] finds an analytical solution for the Marangoni-induced flow of a periodic array, or "flotilla," of identical boats driven purely by surface diffusion of insoluble surfactant in a two-dimensional setting. Even in the simpler two-dimensional setting, and with the same assumptions of zero Reynolds, capillary, and surface Péclet number used by other authors [16,17,21], the relevant problems that incorporate Marangoni effects are challenging mixed boundary value problems requiring proper resolution of the associated contact line stress singularities. The methods of complex analysis can, however, be deployed to great advantage in such two-dimensional problems. For a flotilla of two-dimensional Marangoni boats such methods were used to derive an explicit expression for its collective propulsion speed, as well as an analytical description of the low-Reynolds-number Marangoni-induced flow beneath it [20]. As discussed in that study [20] the solution for propulsion of a single two-dimensional boat driven purely by surface diffusion does not exist, a matter discussed in more detail later.

The present paper is a sequel to the author's previous study [20] and shows how to incorporate reaction effects into that two-dimensional Marangoni boat model. An understanding of reaction effects is important because the latter lead to a removal of surfactants from the interface. When surfactants are deliberately deposited to provide propulsion this removal by sublimation has the useful effect of clearing the surface of surfactant thereby renewing and strengthening surface tension gradients necessary for locomotion. In an experimental study of vapor-driven propulsion on a free surface [22] steady propulsion of a floating boat is achieved through a continuous supply of fuel vapor that lowers the surface tension of the liquid coupled with a spontaneous recovery of the surface tension after the boat has passed caused by evaporation of the surfactant off the interface. To study such a scenario we extend the model of diffusion-driven motion of a flotilla of Marangoni boats [20]. Here, however, we restrict our attention to a single boat but incorporate the additional physical effect of first-order reaction kinetics; this regularizes the two-dimensional problem making a solution possible for a single boat. Using complex analysis techniques, it is demonstrated that a complete analytical description is possible. The strength of the reaction kinetics relative to the surface diffusion of surfactant is measured by a Damköhler number Da. Evidence of the nonexistence of a solution to the single boat problem driven purely by surface diffusion emerges as a singular limit of the new solutions found here as reaction effects vanish in the zero reaction $\mathrm{Da} \to 0$ limit.

Figure 1 shows a schematic of the model. A single Marangoni boat modeled as a thin neutrally buoyant "strip," or plate, of length $2L$ on $y = 0$ in an (x, y) plane floats on a fluid of viscosity μ occupying the lower-half plane $y < 0$. The boat is actuated, for example, by imposing surfactant concentrations $\Gamma^{\pm}$ at its ends that cause a local change in the surface tension, according to a linear

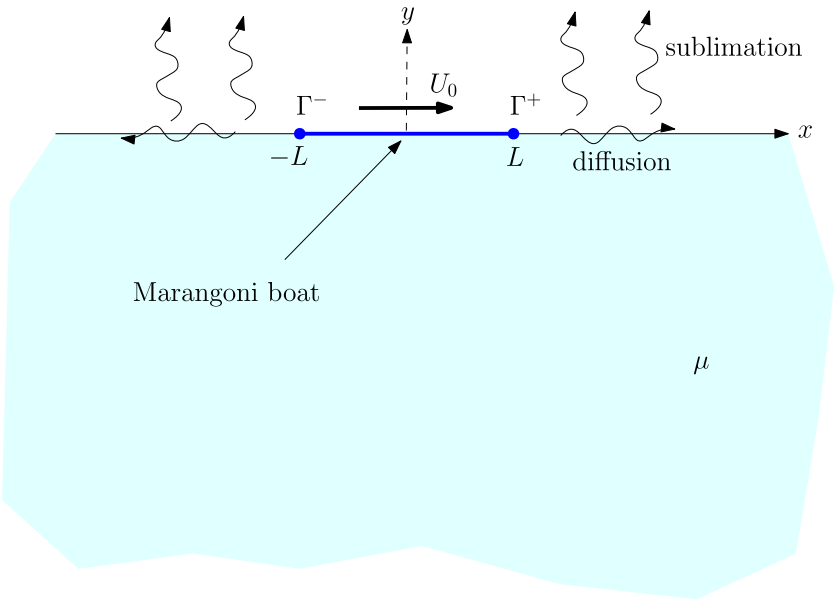

FIG. 1. A Marangoni boat of length $2L$ in an (x, y) plane with surfactant levels $\Gamma^{\pm}$ imposed at its front and rear moves with speed U_0 atop a fluid of viscosity μ due to a surface tension disparity $\Delta\sigma$ caused by the surfactant. The surfactant sublimates to the upper gas phase and diffuses along the interface with the relative strength of these two effects characterized by a Damköhler number Da.

equation of state, and a resulting disparity in surface tension $\Delta\sigma$ across the boat. Under a zero surface Péclet number assumption, once surfactants are deposited on the interface they diffuse along it and sublimate to the ambient gas phase in the upper-half plane $y > 0$. The model is arguably the simplest one possible that captures these physical effects. Despite its simplicity it has an interesting nontrivial solution structure as will be shown

It is useful to summarize the key theoretical results. The speed of the model boat shown in Fig. 1 is found to be

$$U_0 = \frac{\Delta\sigma}{2\pi\mu} e^{\sqrt{\mathrm{Da}}} K_0(\sqrt{\mathrm{Da}}), \qquad \mathrm{Da} \equiv \frac{\alpha L^2}{D}, \qquad \Delta\sigma = \beta(\Gamma^- - \Gamma^+), \tag{1}$$

where Da is a Damköhler number and the material parameter $\beta = RT$ reflects the sensitivity of the surface tension to changes in the surfactant concentration; R is the gas constant and T denotes absolute temperature. The parameters α and D will be explained in Sec. II. K_0 is the modified Bessel function of order zero. The (quasisteady) incompressible Stokes flow beneath the interface is described by the streamfunction

$$\psi(z, \bar{z}) = \mathrm{Im}[(\bar{z} - z) f(z)], \tag{2}$$

where $f(z)$ is given parametrically, in terms of a mathematical parameter ζ, by the explicit expressions

$$f(z) = F(\zeta) \equiv -\frac{\Delta\sigma}{4\mu(1-r)} \left[\frac{e^{\sqrt{\mathrm{Da}}}}{2\pi} \int_{C_L} \frac{d\zeta'}{\zeta'} \frac{\zeta' + \zeta}{\zeta' - \zeta} e^{\sqrt{\mathrm{Da}} X(\zeta')/L} + \frac{r e^{\sqrt{\mathrm{Da}}}}{2\pi} \int_{C_R} \frac{d\zeta'}{\zeta'} \frac{\zeta' + \zeta}{\zeta' - \zeta} e^{-(\sqrt{\mathrm{Da}} X(\zeta')/L)} \right],$$

$$z = Z(\zeta) = \frac{2\zeta L}{\zeta^2 + 1} = X(\zeta) + iY(\zeta), \qquad r = \frac{\Gamma^+}{\Gamma^-}, \qquad \Gamma^- \neq 0, \tag{3}$$

where C_R and C_L denote the right and left halves of the unit circle in a complex ζ plane as sketched later in Fig. 7. As shown in Sec. III variants of the boundary value problem for the surfactant concentration at the edges of the boat can also be solved with only minor adjustments of the scheme. The important special case where the boat is actuated by a surfactant source only at the rear of the boat corresponds to $\Gamma^+ = 0$, or $r = 0$, for which $f(z)$ simplifies to

$$f(z) = F(\zeta) \equiv -\frac{\Delta\sigma}{8\pi\mu} e^{\sqrt{\mathrm{Da}}} \int_{C_L} \frac{d\zeta'}{\zeta'} \frac{\zeta' + \zeta}{\zeta' - \zeta} e^{2\sqrt{\mathrm{Da}}\zeta'/1+\zeta'^2}. \tag{4}$$

The paper is organized as follows. Sections II–IV set out the theoretical model and describe the derivation of the solution summarized in (1)–(3). This involves a reformulation of the Stokes equations in terms of two analytic functions and the derivation of a mixed boundary value problem for one of them; that mixed boundary value problem is solved in Appendix B using conformal mapping methods that fully take account of singularities arising at the contact line. Properties of the solution given in (1)–(3) are analyzed in Sec. V. Section VI provides a complementary view of the problem using the reciprocal theorem and gives a different way to retrieve the same propulsion speed (1). It also leads to a general formula for the propulsion speed useful in other problems involving the same geometrical setup where the Marangoni stress distribution on either side of the boat is determinable. The paper concludes with a discussion in Sec. VII of the implications of the results and possible generalizations.

II. MARANGONI BOAT DRIVEN BY REACTION AND DIFFUSION

Under the assumption that the Reynolds number is zero there is a slow viscous Stokes flow with incompressible velocity $\mathbf{u} = (u, v)$ in the bulk fluid of viscosity μ in the lower-half plane (x, y) as shown in Fig. 1. The governing Stokes equations are

$$\mu\nabla^2\mathbf{u} = \nabla p, \qquad \nabla\cdot\mathbf{u} = 0, \tag{5}$$

where $p(x, y)$ is the fluid pressure. The upper-half region $y > 0$ is occupied by a gas at uniform pressure p_g. In anticipation of finding a boat translating steadily with some speed U_0 in the positive x direction it is expedient to use a frame of reference cotraveling with this *a priori* unknown speed. In this frame the boat occupies the interval $[-L, L]$. The fluid velocity as $y \to -\infty$ is

$$(u, v) \to (-U_0, 0), \qquad \text{as } y \to -\infty. \tag{6}$$

On each portion of the interface the stress induced by the nonuniform surface tension $\sigma(s)$, where s denotes arc length along the boundary taken such that s increases with the fluid region on the left, must be balanced by the fluid stress or [23,24]

$$[\mathbf{T}\cdot\mathbf{n}]^{\text{fluid}}_{\text{gas}} = \sigma\kappa\mathbf{n} - \nabla_s\sigma, \qquad \mathbf{T} \equiv -p\mathbf{I} + \mu\big[\nabla\mathbf{u} + (\nabla\mathbf{u})^T\big], \tag{7}$$

where $\mathbf{T}$ is the fluid stress tensor in either phase, $[\mathbf{T}\cdot\mathbf{n}]^{\text{fluid}}_{\text{gas}}$ denotes the jump in the bracketed quantity between its limit approached from the fluid side and from the gas side, κ is the curvature of the surface, and $\nabla_s = (\mathbf{I} - \mathbf{nn})\cdot\nabla$ denotes the surface gradient on the interface having unit normal $\mathbf{n}$ directed into the fluid. The tangential projection of the boundary condition (7) along the interface gives the Marangoni stress balance

$$\mu\mathbf{t}\cdot\big[\nabla\mathbf{u} + (\nabla\mathbf{u})^T\big]\cdot\mathbf{n} = -\frac{\partial\sigma}{\partial s}. \tag{8}$$

It is this condition that drives the motion of the boat. If a capillary number based on the clean-flow surface tension σ_0 is defined to be

$$\mathrm{Ca} = \frac{\mu U_0}{\sigma_0}, \tag{9}$$

it can be shown [20] by an analysis of the normal component of (7) that as Ca $\to$ 0 it is consistent to seek a solution for a flat interface on either side of the boat where $p_0 = p_g$ where p_g is the uniform gas pressure in $y > 0$ and p_0 denotes the average pressure in the fluid in $y < 0$. The justification is reviewed in Appendix A where the fluid pressure is conveniently decomposed as $p = p_0 + P(x, y)$ where $P(x, y)$ is the deviation from p_0. It is shown there that, for a flat, zero curvature interface, the pressure p_0 must balance the ambient gas pressure p_g. It is also assumed that any surfactant leaving the interface has no effect on the constant pressure gas in $y > 0$ which can be taken to be dynamically inactive.

In summary, in the limit Ca $\to$ 0 the line $y = 0$ is a streamline of the flow. The Marangoni stress balance (8) holds on the interface on each side of the boat. On the boat itself, in the reference frame cotraveling with speed U_0, the no-slip condition

$$(u, v) = (0, 0) \tag{10}$$

holds. At the edges of the boat the fluid velocities must be continuous, but integrable singularities of the fluid stress are expected. The propulsion speed U_0 will be set by the condition that the net force on the boat is zero so that the surface tension force across the boat is balanced by viscous drag.

III. SOLUTION FOR THE SURFACTANT DISTRIBUTION

For a flat interface on $y = 0$ it is natural to view the surface tension distribution as a function of x, $\sigma = \sigma(x)$. It is a common model to take a linear equation of state [20,21,23,24] relating the surfactant concentration $\Gamma(x)$ to the local surface tension value:

$$\sigma(x) = \sigma_0 - \beta\Gamma(x), \tag{11}$$

where β was introduced earlier. This is a good model for moderate surfactant concentrations. By (11) the corresponding surface tension values $\sigma^{\pm}$ at the edges of the boat are

$$\sigma^+ = \sigma_0 - \beta\Gamma^+, \qquad \sigma^- = \sigma_0 - \beta\Gamma^-. \tag{12}$$

Defining $\Delta\sigma \equiv \sigma^+ - \sigma^-$ to be the difference in surface tension across the boat, then

$$\Delta\sigma \equiv \sigma^+ - \sigma^- = -\beta(\Gamma^+ - \Gamma^-). \tag{13}$$

Halpern and Frenkel [25] (see their Appendix B) give a simple derivation of the two-dimensional equation governing the evolution of insoluble surfactant with density $\Gamma(x, t)$ on a two-dimensional interface in an (x, y) plane. For a flat interface $y = 0$ the equation is

$$\frac{\partial}{\partial t}\Gamma + \frac{\partial}{\partial x}(\Gamma u) = D\frac{\partial^2\Gamma}{\partial x^2} - \alpha\Gamma, \qquad \text{on } y = 0, \tag{14}$$

where u is the slip velocity in the x direction on the interface, D is the surface diffusion coefficient, and the final term in (14), not included by Halpern and Frenkel [25], has been added to account for the first-order reaction kinetics associated with sublimation of the surfactant to the gas phase [13,14]. The parameter α is the reaction rate. Nondimensionalizing Γ with respect to Γ^-, lengths with respect to L, velocities with respect to the boat speed U_0, and time with respect to L/U_0, the nondimensional form of (14) is

$$\mathrm{Pe}_s\left[\frac{\partial\Gamma}{\partial t} + \frac{\partial}{\partial x}(\Gamma u)\right] = \frac{\partial^2\Gamma}{\partial x^2} - \mathrm{Da}\Gamma, \qquad \mathrm{Pe}_s \equiv \frac{U_0 L}{D}, \tag{15}$$

where all quantities are now taken to be nondimensional and Pe_s is the surface Péclet number. The Damköhler number, Da, defined in (1) is a ratio of the reaction rate to the surface diffusion rate.

In the limit $\mathrm{Pe}_s \to 0$ where surface diffusion dominates, surface advection equation (15) reduces, in the cotraveling frame, to

$$\frac{d^2\Gamma(x)}{dx^2} - \lambda^2\Gamma = 0, \qquad \lambda^2 = \frac{\alpha}{D}, \qquad |x| > L, \tag{16}$$

where we have reverted to dimensional variables which turn out to be more convenient. The solution to this second-order ordinary differential equation is

$$\Gamma(x) = \begin{cases} \Gamma^- e^{\lambda(L+x)}, & x \leqslant -L \\ \Gamma^+ e^{\lambda(L-x)}, & x \geqslant L. \end{cases} \tag{17}$$

The solution (17) satisfies the far-field condition $\Gamma(x) \to 0$ as $x \to \pm\infty$ meaning that the interface far from the boat is free of surfactant ("clean"), which is physically reasonable since the boat is taken to be the only surfactant source. Solutions will depend on the nondimensional parameter $r = \Gamma^+/\Gamma^-$ introduced in (3). The most common scenario envisaged is that $\Gamma^+ = 0$ with $\Gamma^- > 0$ so that, in order to propel itself in the positive x direction, a boat ejects surfactant from its rear. This is the case $r = 0$. The model, however, allows for any $r \neq 0$. It follows from (17) and (11) that

$$-\frac{\partial \sigma}{\partial x} = \begin{cases} +\beta\lambda\Gamma^- e^{\lambda(L+x)}, & x \leqslant -L \\ -\beta\lambda\Gamma^+ e^{\lambda(L-x)}, & x \geqslant L, \end{cases} \tag{18}$$

which is the gradient of surface tension that drives the motion according to (8).

It is worth mentioning that if, instead of the Dirichlet-type condition on $\Gamma(x)$ at the edges of the boat used above, a Neumann-type boundary condition for the surfactant concentration is used at the edges of the boat, namely,

$$-\frac{d\Gamma}{dx} = \begin{cases} -J^-, & x = -L \\ J^+, & x = +L, \end{cases} \tag{19}$$

where $J^\pm$ denote specified magnitudes of the surfactant fluxes ejected from the edges of the boat, then the analysis to follow is unchanged except for a simple adjustment of the constants, that is, instead of (17) the solution becomes

$$\Gamma(x) = \begin{cases} (J^-/\lambda)e^{\lambda(L+x)}, & x \leqslant -L \\ (J^+/\lambda)e^{\lambda(L-x)}, & x \geqslant L. \end{cases} \tag{20}$$

A mixture of Dirchlet-type and Neumann-type conditions at the two edges of the boat can also be incorporated with similarly minor adjustments of constants.

IV. COMPLEX VARIABLE FORMULATION

The challenge is to solve for the Stokes flow in the lower-half plane $y < 0$ with the mixed boundary conditions on $y = 0$ derived in Sec. II and with the surface tension distribution found in Sec. III. We can introduce the complex variable representation of a biharmonic streamfunction $\psi(z, \bar{z})$ given by [20,23,24]

$$\psi(z,\bar{z}) = \mathrm{Im}[\bar{z}f(z) + g(z)], \qquad (u, v) = \left(\frac{\partial\psi}{\partial y}, -\frac{\partial\psi}{\partial x}\right), \qquad u - iv = 2i\frac{\partial\psi}{\partial z}, \tag{21}$$

where $f(z)$ and $g(z)$ are two functions of $z = x + iy$, having the dimensions of a velocity, that are analytic in $y < 0$ except possibly on $y = 0$ and as $|z| \to \infty$. From the Stokes equations it can be shown that the fluid pressure P, the vorticity $\omega = -\nabla^2\psi = -4\partial^2\psi/\partial z\partial\bar{z}$, and the fluid rate-of-strain tensor $e_{ij} = (1/2)(\partial u_i/\partial x_j + \partial u_j/\partial x_i)$ are related to $f(z)$ and $g(z)$ through

$$4f'(z) = \frac{P}{\mu} - i\omega, \qquad u - iv = -\overline{f(z)} + \bar{z}f'(z) + g'(z), \qquad e_{11} + ie_{12} = z\overline{f''(z)} + \overline{g''(z)}, \tag{22}$$

where primes denote differentiation with respect to z. A derivation of these fundamental relations is given in an Appendix of the study of the Marangoni boat flotilla [20]. There is an additive degree of freedom in the choice of $f(z)$ and $g'(z)$ since the transformations

$$f(z) \mapsto f(z) + c, \qquad g'(z) \mapsto g'(z) + \bar{c}, \tag{23}$$

where $c \in \mathbb{C}$ is a constant do not affect the complex velocity field $u - iv$ given in (22). This degree of freedom will be specified later.

On inspection of (21) it can be checked that the choice

$$g(z) = -zf(z) \tag{24}$$

ensures that $\psi = 0$ on $y = 0$, where $\bar{z} = z$, and renders it a streamline. That this choice is consistent with the far-field requirements and force-free condition on the boat will be verified later. Moreover,

$$g'(z) = -zf'(z) - f(z) \tag{25}$$

so that if $f(z) \mapsto f(z) + c$, then $g'(z) \mapsto g'(z) - c$ implying that the additive degree of freedom c in (23) is now constrained to be purely imaginary. From (22) the complex velocity field, with $g(z)$ given by (24), is

$$u - iv = -\overline{f(z)} + \bar{z}f'(z) + g'(z) = -\overline{f(z)} + (\bar{z} - z)f'(z) - f(z). \tag{26}$$

On $y = 0$, where $\bar{z} = z = x$, it follows from (26) that

$$u - iv = -f(z) - \overline{f(z)} = -2\mathrm{Re}[f(z)]. \tag{27}$$

The boundary condition (10) then implies that on the boat,

$$\mathrm{Re}[f(z)] = 0, \qquad |x| < L, \qquad y = 0. \tag{28}$$

From (6) and (27) the function $f(z)$ must also satisfy the far-field condition in the lower-half plane

$$f(z) \to \frac{U_0}{2} + O(1/z), \qquad \text{as } |z| \to \infty,\ y \leqslant 0, \tag{29}$$

where a possible purely imaginary constant has been set to zero without loss of generality using the available purely imaginary degree of freedom c in (23).

As for the stress condition on the interface, the author has shown elsewhere [20] that the tangential stress condition can be written as

$$\mathrm{Re}\left[2\mu i \frac{dH}{dx}\right] = -\frac{\partial \sigma}{\partial x}, \tag{30}$$

where

$$H(z, \bar{z}) = f(z) + z\overline{f'(z)} + \overline{g'(z)}. \tag{31}$$

If we now use the expression (18) for $-\partial\sigma/\partial x$ derived earlier from the surfactant evolution equation, then

$$\mathrm{Re}\left[2\mu i \frac{dH}{dx}\right] = \begin{cases} +\beta\lambda\Gamma^- e^{\lambda(L+x)}, & x \leqslant -L \\ -\beta\lambda\Gamma^+ e^{\lambda(L-x)}, & x \geqslant L. \end{cases} \tag{32}$$

This can be integrated with respect to x,

$$\mathrm{Im}[2\mu H] = \begin{cases} -\beta\Gamma^- e^{\lambda(L+x)} + \mathrm{Im}[2\mu H^-], & x \leqslant -L \\ -\beta\Gamma^+ e^{\lambda(L-x)} + \mathrm{Im}[2\mu H^+], & x \geqslant L, \end{cases} \tag{33}$$

where two real constants of integration, one on each portion of the interface, have been written as $\mathrm{Im}[2\mu H^{\pm}]$ where

$$H^+ \equiv \lim_{x \to +\infty} [H(x + i0)], \qquad H^- \equiv \lim_{x \to -\infty} [H(x + i0)]. \tag{34}$$

With the choice (24), it can be checked that

$$H = f(x) - \overline{f(x)} = 2i\,\mathrm{Im}[f(x)], \qquad \text{on } y = 0 \tag{35}$$

implying, in order that (33) is consistent with (29) as $|x| \to \infty$, that $H^{\pm} = 0$. Then, combining (33) and (35), it is found that on the interface

$$\mathrm{Im}[f(x)] = \begin{cases} -\dfrac{\beta}{4\mu}\Gamma^{-}e^{\lambda(L+x)}, & x \leqslant -L \\ \\ -\dfrac{\beta}{4\mu}\Gamma^{+}e^{\lambda(L-x)}, & x \geqslant L. \end{cases} \tag{36}$$

The total force (per unit length in the direction perpendicular to the plane of interest) due to surface tension across the entire $y = 0$ line is

$$\sigma(\infty) - \sigma(-\infty). \tag{37}$$

The total force due to viscous stress along it is

$$2\mu i \int_{x=-\infty}^{x=\infty} dH = 2\mu i(H^{+} - H^{-}). \tag{38}$$

But using (35) when adding together (37) and (38) implies that the total force over $y = 0$ is

$$\sigma(\infty) - \sigma(-\infty) - 4\mu(\mathrm{Im}[f(\infty + i0)] - \mathrm{Im}[f(-\infty + i0)]). \tag{39}$$

Since the boundary condition on the interface portions of $y = 0$ is one of local force balance, the sum of the surface tension and viscous drag over these will be zero meaning that (39) is the total force on the boat. For force-free motion, and assuming no other external forces on the boat, the quantity (39) must therefore vanish. The total force (39) is purely real so there is no net force in the y direction; indeed from (22) and (28) it is easy to check that, on the boat, the disturbance pressure from the average $P = 0$ so the normal pressure forces on the boat are in balance and the net torque on it vanishes.

When $\mathrm{Da} \neq 0$ the surfactant evolution equation on the interface tells us that the far-field interface is always rendered clean by reaction effects, i.e.,

$$\sigma(\infty) = \sigma(-\infty) = \sigma_0 \tag{40}$$

implying, from (39), that

$$\mathrm{Im}[f(\infty + i0)] = \mathrm{Im}[f(-\infty + i0)]. \tag{41}$$

This is consistent with the far-field requirement on $f(z)$ that it be lower analytic tending to a constant value in the far field. A solution to the Marangoni boat problem exists in this case.

On the other hand, when $\mathrm{Da} = 0$ (no reaction) the surfactant evolution equation requires that

$$\sigma(\infty) - \sigma(-\infty) = \Delta\sigma \neq 0 \tag{42}$$

since the surfactant concentrations must be (different) constants either side of the boat. Expression (39) then implies

$$4\mu(\mathrm{Im}[f(\infty + i0)] - \mathrm{Im}[f(-\infty + i0)]) = \Delta\sigma \neq 0. \tag{43}$$

This is not consistent with the far-field requirement (29) on $f(z)$ unless $\Delta\sigma = 0$: the solution for force-free motion of the boat with $\Delta\sigma \neq 0$ therefore does not exist when $\mathrm{Da} = 0$. Indeed, a jump in the imaginary part of an analytic function as a point is approached from different directions—in this case, the point at infinity—is the signature of a logarithmic singularity, having a purely real strength, at that point. Indeed, it follows from (43) that we must have

$$f(z) \sim \frac{\Delta\sigma}{4\mu\pi}\log z = \frac{\Delta\sigma}{4\mu\pi}(\ln|z| + i\arg[z]), \qquad \text{as } |z| \to \infty, \tag{44}$$

where log denotes the complex logarithm function since $\arg[z] = 0$ for $z = x > 0$ and $\arg[z] = -\pi$ for $z = x < 0$ where we pass from the positive real axis to the negative x axis through the lower-half

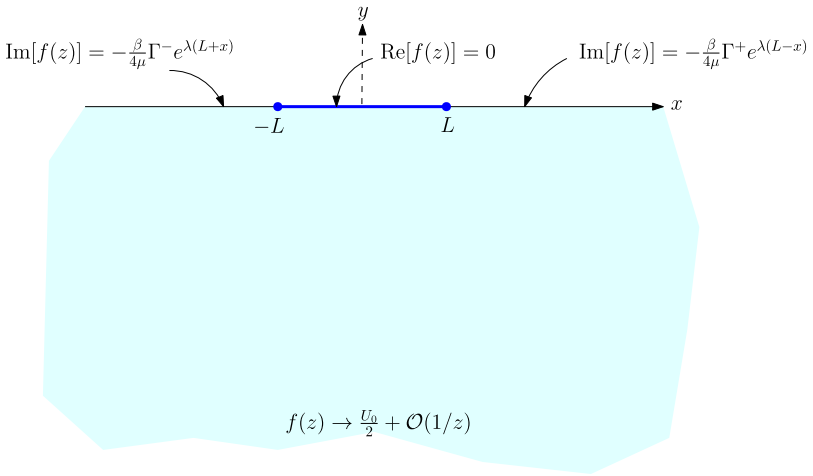

FIG. 2. The mathematical problem for the lower analytic function $f(z)$ to which the physical problem in Fig. 1 is reduced. It is a mixed-type boundary value problem for a lower-analytic function $f(z)$. There are square root branch points in $f(z)$ at $z = \pm L$. The solution can be found using conformal mapping methods as shown in Appendix B.

plane (the fluid region). But the real part of such an $f(z)$ is logarithmically singular as $|z| \to \infty$ and therefore does not tend to a constant value as required in (29).

The same logarithmic divergence of the far-field velocity arises when one tries to satisfy the no-slip condition on a steadily translating body in a two-dimensional Stokes flow: consequently a solution to that "dragging problem" does not exist. This is the familiar Stokes paradox. Indeed it can be shown, using a Schwarz reflection argument to extend the Stokes flow in the $\mathrm{Da} = 0$ Marangoni boat problem in the lower-half plane to a Stokes flow in the entire plane exterior to a finite "plate" (i.e., the boat), that the $\mathrm{Da} = 0$ Marangoni boat problem considered here is mathematically equivalent to the problem of dragging a flat plate (i.e., the boat) along the x axis through an unbounded viscous fluid.

The problem for $\mathrm{Da} \neq 0$ has thus been reduced to a mixed boundary value problem for the lower analytic function $f(z)$ as shown schematically in Fig. 2. The imaginary part of $f(z)$ is a known function, dictated by solution of the surfactant evolution equation, on the two interface portions on $y = 0$ while the real part of $f(z)$ is known to vanish on the boat. This mixed boundary value problem for $f(z)$ can be solved explicitly using conformal mapping methods; the details can be found in Appendix B with the results of that analysis reported in (1)–(3). The following section explores features of the solutions.

V. CHARACTERIZATION OF THE SOLUTIONS

Figure 3 shows a graph of $U_0(2\pi\mu)/\Delta\sigma$ against Damköhler number Da. The propulsion velocity of the boat becomes unbounded as $\mathrm{Da} \to 0$ when reaction effects become unimportant. Indeed, as $\mathrm{Da} \to 0$ it follows from (1) and the known behavior [26]

$$K_0(\sqrt{\mathrm{Da}}) \sim -\ln\sqrt{\mathrm{Da}} \tag{45}$$

that

$$U_0 \sim -\frac{\Delta\sigma}{2\pi\mu}\ln\sqrt{\mathrm{Da}}, \qquad \text{as } \mathrm{Da} \to 0. \tag{46}$$

The boat speed therefore becomes logarithmically unbounded as reaction effects vanish. This singular limit is a manifestation of the nonexistence of a solution, as just discussed, to the model

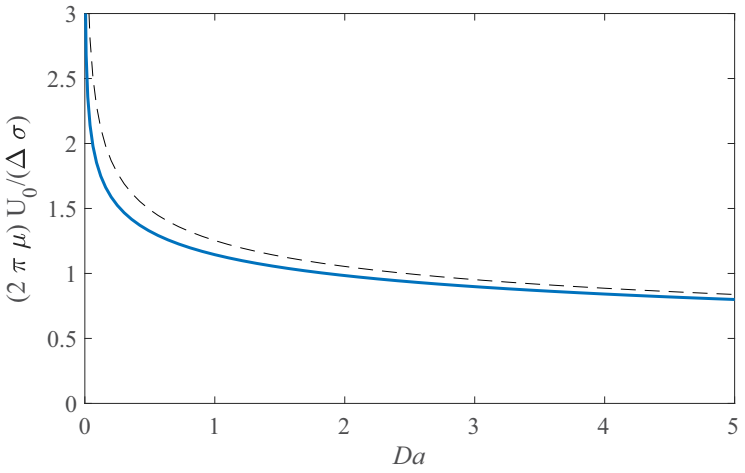

FIG. 3. Graph of $U_0(2\pi\mu)/\Delta\sigma$ against Da. The dashed line is the asymptote $\sqrt{\pi/2}(\mathrm{Da})^{-1/4}$.

problem when $\mathrm{Da} = 0$. The analysis indicates that the presence of nonzero Marangoni stresses on the interface due to reaction effects, i.e., $\mathrm{Da} > 0$, can regularize the problem. This result is consistent with a similar result in the single-boat limit of the flotilla analysis [20] where the same logarithmic singularity in the propulsion speed emerges as the period of the arrangement tends to infinity. Just as periodicity regularized the nonexistent single-boat limit there, that is, consideration of a periodic flotilla of boats rather than just a single boat, here it is reaction effects that provide the regularization mechanism for nonzero Da.

In the opposite limit $\mathrm{Da} \to \infty$, where reaction effects dominate, the fact [26] that

$$K_0(\sqrt{\mathrm{Da}}) \sim \sqrt{\frac{\pi}{2\sqrt{\mathrm{Da}}}} e^{-\sqrt{\mathrm{Da}}} \tag{47}$$

can be used to deduce from (1) that

$$U_0 \sim \frac{\Delta\sigma}{2\pi\mu}\sqrt{\frac{\pi}{2}}\frac{1}{\mathrm{Da}^{1/4}}, \qquad \text{as } \mathrm{Da} \to \infty. \tag{48}$$

There is a slow algebraic decay of propulsion speed with increasing Da. In this limit surfactant sublimates off the interface so readily after it is emitted from the boat that the driving mechanism for Marangoni propulsion eventually becomes ineffective.

Figure 3 reveals that U_0 increases dramatically only for small Da, it decays slowly, like $\mathrm{Da}^{-1/4}$, for large Da, and there is a large intermediate range of Da where the propulsion speed does not vary appreciably. In an experimental study of vapor-driven propulsion on a free surface [22], the propulsion speed of the boat is found to be relatively insensitive to changes in operating conditions. Those observations are qualitatively consistent with the theoretical evidence in Fig. 3. The boat speed is also always positive, and this is consistent with previous analyses [16] where disk-shaped boats are found to always travel in the expected direction. Reverse Marangoni propulsion is believed to be associated with regions of negative pressure on the boat [15] and, as mentioned earlier, the pressure forces on the flat boat in the present setup vanish so any such mechanism for reverse propulsion is absent.

Given the explicit form (2)-(3) for the streamfunction, its contours, that is, the streamlines, are readily examined for different parameters. When $r = 1$ an equal amount of surfactant is ejected at the front and rear of the boat. The associated speed of propulsion $U_0 = 0$ since the Marangoni flow generated by the surfactant is symmetric about the center of the boat. Until this left-right symmetry is broken, no propulsion of the boat is expected in this zero surface Péclet number

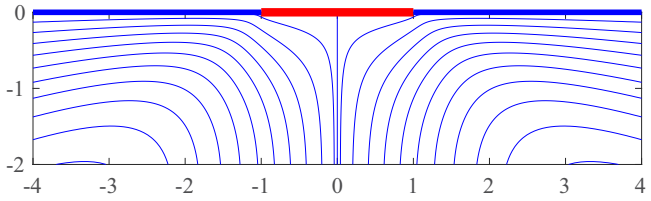

FIG. 4. Fore-aft symmetric eddy structure beneath the boat when Da $= 1$ and $r = 1$ so that equal amounts of surfactant are ejected both fore and aft. The flow induced by the Marangoni stress is symmetric about the center of the boat which consequently remains stationary: $U_0 = 0$.

regime. Figure 4 confirms that the streamline distribution for Da $= 1$ and $r = 1$ has the anticipated symmetry. Although the boat is not moving, there is nevertheless a nontrivial recirculatory flow beneath it driven by the Marangoni stress. The lower surface tension near the edges of the boat compared to the value in the far field means that a fore-aft symmetric eddy pair is set up whereby fluid is dragged out along the interface away from the boat towards remote areas with higher surface tension. There must be a compensating upwelling of fluid towards the boat in the y direction leading to the observed eddy structure.

Besides Da and μ, the propulsion speed U_0 depends only on the surface tension disparity $\Delta\sigma$ across the boat. The latter, in turn, depends only on the difference $\Gamma^- - \Gamma^+$ and the constant β. For fixed μ and β there is, for any choice of Da, a one-parameter family, parametrized by r, of *different* flows associated with the *same* boat propulsion speed U_0. To investigate this it is convenient to assume $\Gamma^- \neq 0$ and to set

$$\Gamma^+ = \frac{r}{1-r}, \qquad \Gamma^- = \frac{1}{1-r}, \qquad 0 \leqslant r < 1 \tag{49}$$

so that $r = \Gamma^+/\Gamma^-$ parametrizes a family of solutions for which the propulsion speed U_0 is fixed since $\Gamma^- - \Gamma^+ = 1$ for any choice of r. Only the range $0 \leqslant r < 1$ is of interest for the following reasons. First, $r > 0$ since it is a ratio of (positive) surfactant concentrations. With the parametrization (49), $r = 1$ is not allowed but this corresponds to the symmetric case shown in Fig. 4 that has just been discussed. Finally, any $r > 1$ corresponds to exchanging the roles of Γ^- and Γ^+ and offers no new information—the boat will merely move to the left instead.

Figure 5 shows the streamline distributions, both in the fixed and cotraveling frames, for fixed Da $= 1$ and four values of r decreasing from unity: $r = 0.75,\ 0.5,\ 0.25,$ and 0. The boat speed U_0 is the *same* for all cases shown, yet the streamline topologies are quite different. As r decreases from unity, the quantity of surfactant emitted at the front of the boat relative to its rear decreases until, at $r = 0$, no surfactant is emitted there at all. The symmetry breaking is most evident in the cotraveling frame where the effect on the symmetric eddy structure in Fig. 4 can be readily tracked. As r decreases the eddy near the rear of the boat at $x = -L$ increases in size while that near the front of the boat at $x = L$ becomes more compact until, eventually, it is no longer visible when $r = 0$. An eddy is only visible in the fixed reference frame, near the front of the boat, when r is close to unity. Figure 6 shows streamlines for the same set of r values but for Da $= 10$ so that sublimation off the interface is stronger.

VI. A RECIPROCAL THEOREM FOR A 2D MARANGONI BOAT

In view of previous work [16,17] where reciprocal theorems for Marangoni propulsion have been deployed in the three-dimensional case under the same assumptions of zero Reynolds and capillary numbers adopted here, it is of interest to ask if there is an analogous result in the two-dimensional setting. The answer is in the affirmative: it is demonstrated in Appendix C how the

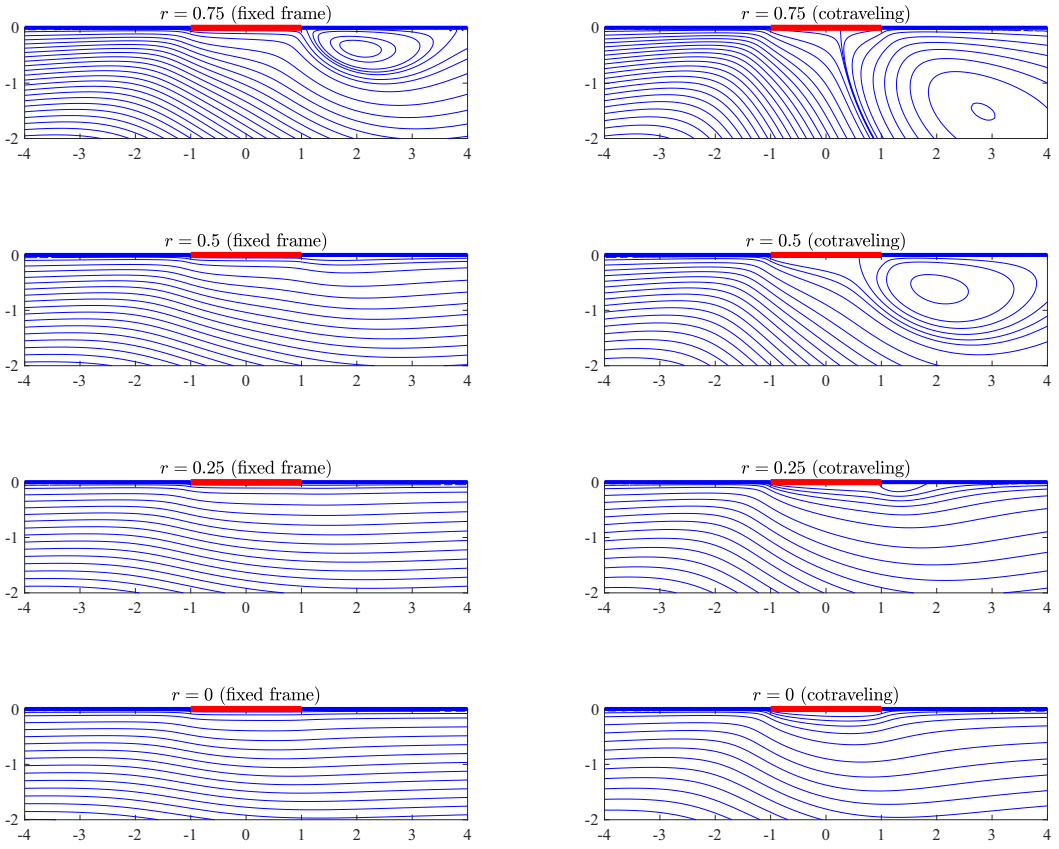

FIG. 5. Streamlines in the fixed frame (left column) and the cotraveling frame (right column) for Da = 1 and $r = 0.75$ (top row), 0, 5, 0.25, and 0 (bottom row). The case $r = 0$ corresponds to actuation at the rear only. The boat propulsion speed U_0 is identical in all cases shown although the streamline topology changes dramatically with r.

reciprocal theorem for Stokes flow can be used to deduce that

$$U_0 = -\frac{1}{2\pi\mu}\left[\int_{-\infty}^{-L} \ln\left|\frac{x-\sqrt{x^2-L^2}}{L}\right|\frac{\partial\sigma}{\partial x}dx + \int_{L}^{\infty} \ln\left|\frac{x-\sqrt{x^2-L^2}}{L}\right|\frac{\partial\sigma}{\partial x}dx\right]. \tag{50}$$

This is a general formula: it can be used to compute the boat speed in any such Marangoni flow problem where a determination of $\partial\sigma/\partial x$ is possible. In Appendix C it is also verified that the earlier result (1) for U_0 can be retrieved from (50) thereby providing a consistency check on the analysis. It is important to note that formula (50) is derived *assuming* a solution to the force-free Marangoni boat problem exists. In the reaction-diffusion Marangoni boat problem considered here, when Da = 0 a solution when $\Delta\sigma \neq 0$ does not exist meaning that (50) does not apply.

VII. DISCUSSION

A simple model problem of a Marangoni boat propelled by surface diffusion and sublimation of insoluble surfactant has been presented and solved using complex variable methods. The boat propulsion speed is given by formula (1); the streamfunction associated with the flow driven in the bulk viscous fluid can be represented as an explicit integral (2)-(3). Such formulas make it easy to

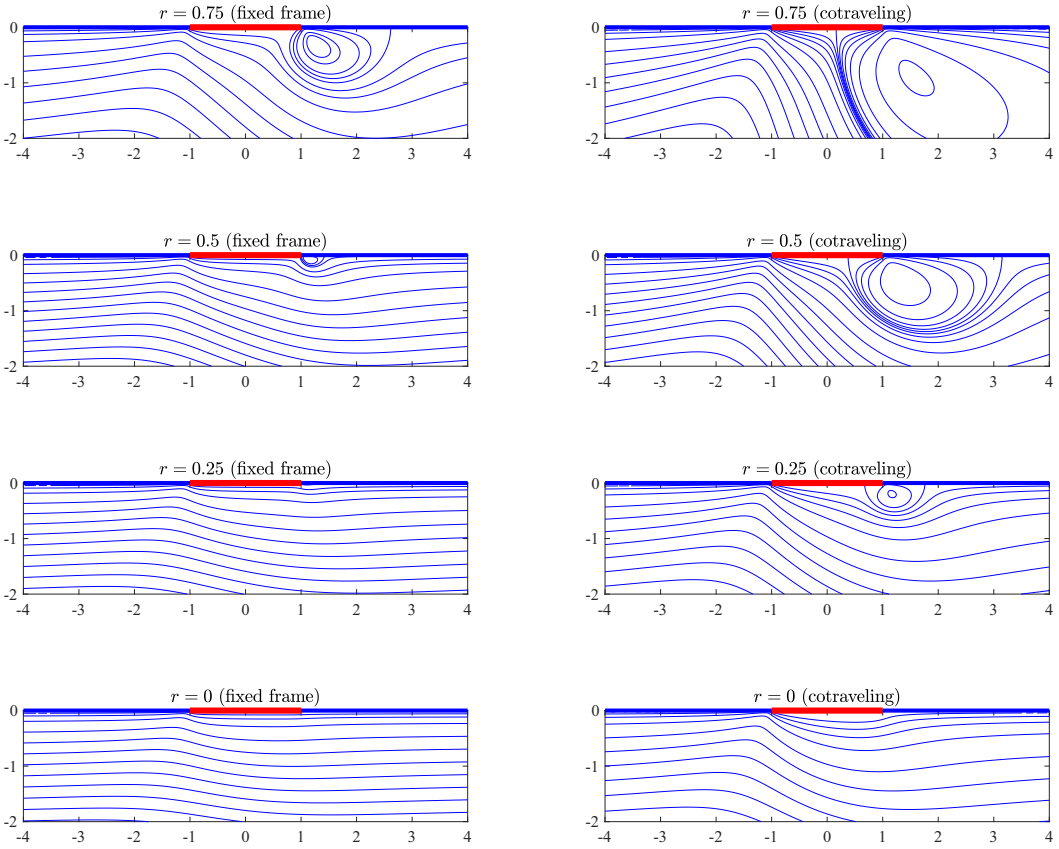

FIG. 6. Streamlines in the fixed frame (left column) and the cotraveling frame (right column) for Da $= 10$ and $r = 0.75$ (top row), 0, 5, 0.25, and 0 (bottom row). The case $r = 0$ corresponds to actuation at the rear only. The boat propulsion speed U_0 is identical in all cases shown.

study streamline topologies and other solution features. Solutions to variants of this problem can be found by simple adjustments of the methodology.

The new solutions can be viewed as a form of solitary traveling wave caused by the localized emission of surfactant driving a Marangoni-induced flow in the bulk viscous fluid. By extension, a previous analysis of a flotilla of Marangoni boats [20] driven purely by surface diffusion and also available in closed form, can be viewed as periodic traveling waves. By a combination of the mathematical ideas presented here and in the study of the flotilla [20], analytical progress on finding the collective speed of a Marangoni boat flotilla when both surface diffusion and first-order reaction kinetics are present is also possible. The details remain to be worked out but, in view of the present and former [20] studies, such an analysis is a routine extension.

Analytical solutions of such multiphysics problems are rare but valuable. While the direct physical applicability of two-dimensional models is limited, their tractability compared with the three-dimensional case facilitates theoretical examination of physical effects which, in many instances, are likely to be qualitatively similar in three dimensions. A perturbative approach, using the analytical solutions here as a base state, is an obvious strategy for incorporating additional physical effects and has been illuminating in recent studies of other problems [27,28]. This is particularly important in multiphysics settings where, in just a partial list, additional physical effects here might include weak solubility in the bulk, small Péclet number effects (both surface and bulk), small capillary number effects and interface deflection, higher-order reaction kinetics or modeling of

multiple species, small inertia effects, and unsteadiness either in the surfactant evolution equation, or the hydrodynamics, or both. Use of domain perturbation techniques is expected to allow the study of propulsion of boats of different shapes including nonflat surfers such as those studied in [15–17], as well as finite-depth effects [15]. The availability of analytical solutions is also valuable when combined with reciprocal theorems. Useful information about solutions to new problems can often be gleaned by using these integral identities together with exact solutions to known problems [17,27,29]. The result of Sec. VI using an exact solution given in (C2) of Appendix C is an example of precisely this. Deployment of the new analytical solution (1)–(3) in reciprocal identities may similarly lead to other new results.

Conformal mapping methods akin to those deployed here have proven to be useful in solving other mixed boundary value problems arising in studies of the effects of reaction kinetics on the self-propulsion of so-called Janus particles driven not by Marangoni stresses but by slip velocities caused by solute dissolution into the bulk ambient fluid [30,31]. As here, the methods led to an explicit formula for the particle velocity in that problem too.

APPENDIX A: ZERO CAPILLARY NUMBER ASSUMPTION

Suppose the pressure in the fluid is denoted by

$$p(x, y) = p_0 + P(x, y), \tag{A1}$$

where p_0 is the average fluid pressure on the interface and $P(x, y)$ is the deviation from this average value. On each portion of the interface (7) says that the stress induced by the nonuniform surface tension must be balanced by the fluid stress [23,24]. From the Marangoni stress balance (8) we expect the boat speed U_0 to scale with the jump in surface tension $\Delta\sigma$ across it:

$$U_0 \sim \frac{\Delta\sigma}{\mu}. \tag{A2}$$

The normal component of (7) is

$$-(p_0 - p_g) - P(x, y) + \mu\mathbf{n} \cdot \left[\nabla\mathbf{u} + (\nabla\mathbf{u})^T\right] \cdot \mathbf{n} = \kappa[\sigma_0 - \beta\Gamma(x)]. \tag{A3}$$

If we nondimensionalize the pressure disturbance $P(x, y)$ with respect to $\mu U_0/L$, lengths with respect to L, and $\beta\Gamma(x)$ with respect to $\Delta\sigma$, (A3) can be written as

$$-\frac{(p_0 - p_g)L}{\sigma_0} + \mathrm{Ca}\left[-\hat{P}(x, y) + \mathbf{n} \cdot \left[\nabla\hat{\mathbf{u}} + (\nabla\hat{\mathbf{u}})^T\right] \cdot \mathbf{n}\right] = \hat{\kappa}\left(1 - \frac{\Delta\sigma}{\sigma_0}\hat{\beta}\hat{\Gamma}(x)\right), \tag{A4}$$

where hats denote nondimensional quantities and the capillary number based on the clean-flow interface surface tension is defined in (9). The final term of (A4) can be seen to be of order Ca since, on use of (A2),

$$\frac{\Delta\sigma}{\sigma_0} \sim \mathrm{Ca}. \tag{A5}$$

If $\mathrm{Ca} \ll 1$ the dominant terms in the normal stress balance (A4) require

$$-\frac{(p_0 - p_g)L}{\sigma_0} = \hat{\kappa}. \tag{A6}$$

A constant curvature interface is therefore a consistent solution in this small capillary number limit. For the flat surface of interest here $\hat{\kappa} = 0$ and we must have $p_0 = p_g$. For this flat interface to be a consistent equilibrium it must be a streamline of the flow.

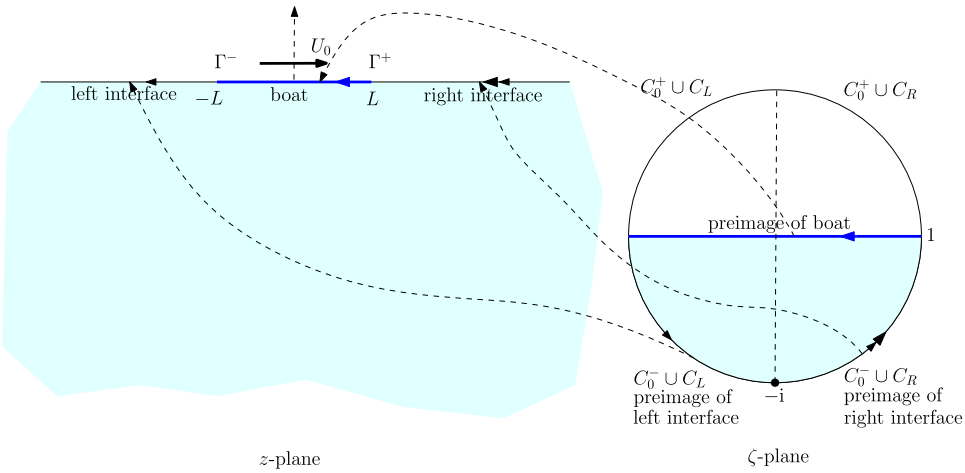

FIG. 7. Conformal mapping (B1) from the lower-half unit disk in a complex ζ plane to the fluid region $y < 0$ below the Marangoni boat. The point $\zeta = -i$ is the preimage of the point at infinity in the lower-half z plane $y \to -\infty$. The preimage of the boat is the real diameter $\zeta \in (-1, 1)$. Tracing arrows around the boundaries in each plane shows the correspondences under (B1).

APPENDIX B: SOLUTION BY CONFORMAL MAPPING

To solve for the flow we will employ conformal mapping techniques. Let

$$z = Z(\zeta) = \frac{2\zeta L}{\zeta^2 + 1} = X(\zeta) + iY(\zeta). \tag{B1}$$

This conformal mapping is the reciprocal of the well-known Joukowski mapping, $(1/2)(\zeta + \zeta^{-1})$, to a flat-plate airfoil familiar in aerodynamics [32,33]. The mapping (B1) transplants the lower-half unit disk in a complex ζ plane to the fluid region in the lower-half plane $y < 0$, with the real diameter $\zeta \in (-1, 1)$ corresponding to the boat and the lower-half unit circle, denoted by C_0^-, corresponding to the interface. The point $\zeta = -i$ is the preimage of the point at infinity in the lower-half complex z plane. Figure 7 shows a schematic of the mapping and the boundary correspondences under it.

To see which parts of C_0^- correspond to the left and right portions of the interface it is convenient to give names to four "halves" of the unit ζ circle: C_0^+ and C_0^- will denote the upper-half and lower-half unit ζ circles; C_R and C_L will denote the right-half and left-half unit ζ circles. This means, for example, that $C_0^+ \cup C_R$ denotes the portion of the unit ζ circle in the first quadrant; the three other quadrants have similar designations as indicated in Fig. 7. Under the mapping (B1) the segment $C_0^- \cup C_R$ is transplanted to the interface on the positive real axis on the right of the boat in Fig. 7; $C_0^- \cup C_L$ is transplanted to the interface on the negative real axis on the left of the boat.

It is useful to introduce the function $h(z)$ defined via

$$f(z) = -\frac{i\beta}{4\mu} h(z), \tag{B2}$$

together with this function composed with the conformal mapping, namely,

$$\mathcal{H}(\zeta) \equiv h(Z(\zeta)). \tag{B3}$$

The function $\mathcal{H}(\zeta)$ is known to be analytic in the lower-half unit ζ disk. We now employ some useful manipulations used by the author in other problems [23,32] where a similar mathematical structure pertains. On the real diameter $\zeta \in (-1, 1)$, which corresponds to the boat, we have $\overline{\zeta} = \zeta$

and it follows from (28) that

$$\mathrm{Im}[\mathcal{H}(\zeta)] = 0, \qquad \text{or} \qquad \overline{\mathcal{H}}(\zeta) = \mathcal{H}(\zeta), \tag{B4}$$

where the Schwarz conjugate $\overline{p}(\zeta)$ of an analytic function $p(\zeta)$ is defined by $\overline{p}(\zeta) \equiv \overline{p(\overline{\zeta})}$. We can infer from (B4), using the Schwarz reflection principle [34], that $\mathcal{H}(\zeta)$ is also analytic in the upper-half unit disk $|\zeta| < 1$, implying that it is analytic in the entire unit disk. On C_0^-, which corresponds to the interface, it follows from (36) that

$$\mathrm{Re}[\mathcal{H}(\zeta)] = \begin{cases} \Gamma^- e^{\lambda[L+X(\zeta)]}, & \zeta \text{ on } C_0^- \cup C_L \\ \Gamma^+ e^{\lambda[L-X(\zeta)]}, & \zeta \text{ on } C_0^- \cup C_R. \end{cases} \tag{B5}$$

Suppose now that $\zeta \in C_0^+ \cup C_R$, then $\overline{\zeta} \in C_0^- \cup C_R$; similarly, if $\zeta \in C_0^+ \cup C_L$, then $\overline{\zeta} \in C_0^- \cup C_L$. Therefore, for any $\zeta \in C_0^+$, that is, any point on the *upper*-half unit ζ circle, we have

$$\mathrm{Re}[\mathcal{H}(\zeta)] = \mathrm{Re}[\overline{\mathcal{H}(\zeta)}] = \mathrm{Re}[\mathcal{H}(\overline{\zeta})] = \begin{cases} \Gamma^- e^{\lambda[L+X(\overline{\zeta})]}, & \overline{\zeta} \text{ on } C_0^- \cup C_L \\ \Gamma^+ e^{\lambda[L-X(\overline{\zeta})]}, & \overline{\zeta} \text{ on } C_0^- \cup C_R, \end{cases} \tag{B6}$$

where the first equality follows because the real parts of complex conjugate quantities are equal, the second equality follows from (B4), and the third equality follows from (B5). If $\overline{\zeta} \in C_0$, then $\overline{\zeta} = 1/\zeta$ and it is easy to check that

$$X(\overline{\zeta}) = X(1/\zeta) = Z(1/\zeta) = Z(\zeta) = X(\zeta) \tag{B7}$$

implying, from (B6), that

$$\mathrm{Re}[\mathcal{H}(\zeta)] = \begin{cases} \Gamma^- e^{\lambda[L+X(\zeta)]}, & \zeta \text{ on } C_0^+ \cup C_L \\ \Gamma^+ e^{\lambda[L-X(\zeta)]}, & \zeta \text{ on } C_0^+ \cup C_R. \end{cases} \tag{B8}$$

Together (B5) and (B8) imply that

$$\mathrm{Re}[\mathcal{H}(\zeta)] = \begin{cases} \Gamma^- e^{\lambda[L+X(\zeta)]}, & \zeta \text{ on } C_L \\ \Gamma^+ e^{\lambda[L-X(\zeta)]}, & \zeta \text{ on } C_R. \end{cases} \tag{B9}$$

Since $C_L \cup C_R$ makes up the entire unit ζ circle, the mathematical problem for $\mathcal{H}(\zeta)$ has thus been reduced to a standard boundary value problem known as the Schwarz problem in the unit disk [32,35]: that of finding a function $\mathcal{H}(\zeta)$ analytic in $|\zeta| < 1$ given its real part everywhere on the boundary $|\zeta| = 1$. The solution is furnished by the Poisson integral formula [32,34,35]

$$\mathcal{H}(\zeta) = \frac{1}{2\pi i}\int_{C_L} \frac{d\zeta'}{\zeta'}\frac{\zeta'+\zeta}{\zeta'-\zeta}\Gamma^- e^{\lambda[L+X(\zeta')]} + \frac{1}{2\pi i}\int_{C_R} \frac{d\zeta'}{\zeta'}\frac{\zeta'+\zeta}{\zeta'-\zeta}\Gamma^+ e^{\lambda[L-X(\zeta')]}, \tag{B10}$$

where a possible additive imaginary constant has been set to zero to ensure that (B4) holds. With the use of (B2) and (16) the integral expression (B10) leads to the result (3) reported earlier. For values of ζ on the unit circle evaluation of the Cauchy-type integrals (B10) can be performed in the usual way (e.g., with the use of the Plemelj formulas [34]).

To find the speed U_0 of the boat (29) can be used. It implies that

$$\frac{U_0}{2} = \lim_{y\to-\infty} \mathrm{Re}[f(z)] = \frac{\beta}{4\mu}\lim_{\zeta\to -i} \mathrm{Im}[\mathcal{H}(\zeta)], \tag{B11}$$

where we have used (B2) and (B3) and the fact that $\zeta = -i$ is the preimage of infinity in the lower-half z plane. From (B10), and the Plemelj formula [34], it follows that

$$\mathcal{H}(-i) = \frac{\Gamma^- e^{\lambda L}}{2\pi i}\fint_{C_L} \frac{d\zeta'}{\zeta'}\frac{\zeta'-i}{\zeta'+i} e^{\lambda X(\zeta')} + \frac{\Gamma^+ e^{\lambda L}}{2\pi i}\fint_{C_R} \frac{d\zeta'}{\zeta'}\frac{\zeta'-i}{\zeta'+i} e^{-\lambda X(\zeta')}, \tag{B12}$$

where $\fint$ refers to a principal part integral. Owing to the exponential decay of the integrand as $\zeta' \to -i$ these principal part integrals require no special treatment. On setting $\zeta' = e^{i\theta}$ it can be

shown that

$$\frac{\zeta'-i}{\zeta'+i}=\frac{e^{i\theta}-i}{e^{i\theta}+i}=-\frac{i\cos\theta}{1+\sin\theta},\qquad X(\zeta')=L\sec\theta. \tag{B13}$$

The use of these in (B12) leads to

$$\mathcal{H}(-i)=-\frac{i}{2\pi}\left[\Gamma^{+}e^{\lambda L}\int_{-\pi/2}^{\pi/2}\frac{\cos\theta}{1+\sin\theta}e^{-\lambda L\sec\theta}d\theta+\Gamma^{-}e^{\lambda L}\int_{\pi/2}^{3\pi/2}\frac{\cos\theta}{1+\sin\theta}e^{+\lambda L\sec\theta}d\theta\right]. \tag{B14}$$

With use of the substitution $\theta=\pi-\phi$ in its second integral (B14) simplifies to

$$\mathcal{H}(-i)=-\frac{i}{2\pi}(\Gamma^{+}e^{\lambda L}-\Gamma^{-}e^{\lambda L})\mathcal{I}(\lambda L),\qquad \mathcal{I}(\lambda L)\equiv\int_{-\pi/2}^{\pi/2}\frac{\cos\theta}{1+\sin\theta}e^{-\lambda L\sec\theta}d\theta. \tag{B15}$$

Combining this with (B11) yields

$$U_0=\frac{\Delta\sigma}{4\pi\mu}e^{\lambda L}\mathcal{I}(\lambda L), \tag{B16}$$

where, in the last equality, we have used (13). The quantity $\mathcal{I}(\lambda L)$ can be identified with a modified Bessel function. To see this, note that

$$\mathcal{I}(\lambda L)=\int_{-\pi/2}^{\pi/2}\frac{\cos\theta(1-\sin\theta)}{1-\sin^2\theta}e^{-\lambda L\sec\theta}d\theta=\int_{-\pi/2}^{\pi/2}\frac{(1-\sin\theta)}{\cos\theta}e^{-\lambda L\sec\theta}d\theta \tag{B17}$$

or, since the odd part of the integrand will give zero contribution to the integral,

$$\mathcal{I}(\lambda L)=\int_{-\pi/2}^{\pi/2}\frac{e^{-\lambda L\sec\theta}}{\cos\theta}d\theta=2\int_{0}^{\pi/2}\frac{e^{-\lambda L\sec\theta}}{\cos\theta}d\theta=2\int_{1}^{\infty}\frac{e^{-\lambda Lu}}{\sqrt{u^2-1}}du, \tag{B18}$$

where we have introduced the change of variable $u=\sec\theta$. Another change of integration variable $u=\cosh w$ leads to

$$\mathcal{I}(\lambda L)=2\int_{0}^{\infty}e^{-\lambda L\cosh w}dw=2K_0(\lambda L), \tag{B19}$$

where, in the second equality, we have recognized an integral representation of the zeroth-order modified Bessel function $K_0(\lambda L)$ [26]. The speed of the boat is therefore (1) where we have used the fact, following from (1) and (16), that $\lambda L=\sqrt{\mathrm{Da}}$.

APPENDIX C: DERIVATION OF PROPULSION SPEED FORMULA (50)

If D is a two-dimensional fluid domain and ∂D its boundary, then the reciprocal theorem says

$$\int_{\partial D}u_i\hat{\sigma}_{ij}n_j ds=\int_{\partial D}\hat{u}_i\sigma_{ij}n_j ds, \tag{C1}$$

where $\{u_i,\sigma_{ij}\}$ and $\{\hat{u}_i,\hat{\sigma}_{ij}\}$ are two solutions of the Stokes equations in D and ds denotes the arc-length element around the boundary. Let $\{u_i,\sigma_{ij}\}$ be the solution of the $\mathrm{Da}\neq 0$ Marangoni boat problem in the lower-half plane considered here and let $\{\hat{u}_i,\hat{\sigma}_{ij}\}$ be the Stokes flow in the same domain associated with the functions

$$\hat{f}(z)=\log\left(\frac{z-\sqrt{z^2-L^2}}{L}\right),\qquad \hat{g}(z)=-z\hat{f}(z), \tag{C2}$$

where log is the complex logarithm function.

To apply the reciprocal theorem (C1) to the Marangoni boat problem we want to pick D to be the lower-half plane. We will consider this as a limit of a set of domains D_R with boundary ∂D_R taken to be $C_R\cup(-R,R)$ where C_R is a semicircle of radius R in the lower-half plane meeting the real axis

at $(\pm R, 0)$; the lower-half plane is approached in the limit $R \to \infty$. In this section we will work in a fixed frame of reference in which the boat instantaneously occupies the interval $[-L, L]$ and moves with speed U_0.

In complex variable notation, for any $R > 0$, (C1) becomes

$$\int_{\partial D_R} \mathrm{Re}\left[(u - iv)\left(-2\mu i \frac{d\hat{H}}{ds}\right)\right] ds = \int_{\partial D_R} \mathrm{Re}\left[(\hat{u} - i\hat{v})\left(-2\mu i \frac{dH}{ds}\right)\right] ds, \tag{C3}$$

where

$$H = f(z) + z\overline{f'(z)} + \overline{g'(z)}, \qquad \hat{H} = \hat{f}(z) + z\overline{\hat{f}'(z)} + \overline{\hat{g}'(z)}. \tag{C4}$$

On letting $R \to \infty$ it can be checked using the far-field conditions on the Marangoni boat problem that any contributions to the integrals in (C3) from C_R vanish leading to

$$\int_{-\infty}^{\infty} \mathrm{Re}\big[(u - iv)\big(-2\mu i d\hat{H}\big)\big] = \int_{-\infty}^{\infty} \mathrm{Re}[(\hat{u} - i\hat{v})(-2\mu i dH)]. \tag{C5}$$

It is known from (27) and (35) that any Stokes flow for which $g(z) = -zf(z)$ satisfies, on $y = 0$,

$$u - iv = -2\,\mathrm{Re}[f(z)], \qquad H = 2i\,\mathrm{Im}[f(z)] \tag{C6}$$

and similar relations hold for the hatted flow associated with the choice (C2). Thus (C5) can be written as

$$\int_{-\infty}^{\infty} \mathrm{Re}[f(x)] d\,\mathrm{Im}\big[\hat{f}(x)\big] = \int_{-\infty}^{\infty} \mathrm{Re}\big[\hat{f}(x)\big] d\,\mathrm{Im}[f(x)]. \tag{C7}$$

Now the convenient properties of the special choice (C2) appear. It is easy to verify, directly from (C2), that

$$\mathrm{Im}[\hat{f}(x)] = \begin{cases} 0, & x \geqslant L \\ -\pi, & x \leqslant -L, \end{cases} \tag{C8}$$

while

$$\mathrm{Re}[\hat{f}(x)] = 0, \qquad |x| \leqslant L. \tag{C9}$$

The integral on the left-hand side of (C7) therefore reduces to

$$\int_{-L}^{L} \mathrm{Re}[f(x)] d\,\mathrm{Im}\big[\hat{f}(x)\big] = -\frac{U_0}{2} \int_{-L}^{L} d\,\mathrm{Im}\big[\hat{f}(x)\big] = -\frac{U_0 \pi}{2} \tag{C10}$$

so that (C7) gives the result

$$U_0 = -\frac{2}{\pi}\left[\int_{-\infty}^{-L} \mathrm{Re}\big[\hat{f}(x)\big] \frac{d\,\mathrm{Im}[f(x)]}{dx} dx + \int_{L}^{\infty} \mathrm{Re}\big[\hat{f}(x)\big] \frac{d\,\mathrm{Im}[f(x)]}{dx} dx\right]. \tag{C11}$$

But it follows from (30) and (35) that

$$\frac{d}{dx}\mathrm{Im}[f(x)] = \frac{1}{4\mu}\frac{\partial \sigma}{\partial x}, \tag{C12}$$

therefore

$$U_0 = -\frac{1}{2\pi\mu}\left[\int_{-\infty}^{-L} \mathrm{Re}\big[\hat{f}(z)\big] \frac{\partial \sigma}{\partial x} dx + \int_{L}^{\infty} \mathrm{Re}\big[\hat{f}(z)\big] \frac{\partial \sigma}{\partial x} dx\right]. \tag{C13}$$

This is the required formula.

The general result (50), or equivalently (C11), can be used to check the result for U_0 obtained by solving the full boundary value problem. Performing integration by parts on the integral on the

right-hand side of (C11), and use of (C2), leads to

$$U_0 = \frac{2}{\pi}\left[\int_{-\infty}^{-L} \mathrm{Im}[f(z)]d\,\mathrm{Re}\big[\hat{f}(z)\big] + \int_{L}^{\infty} \mathrm{Im}[f(z)]d\,\mathrm{Re}\big[\hat{f}(z)\big]\right]. \tag{C14}$$

For $|x| > L$ it also follows from (C2) that

$$d\hat{f} = -\frac{dx}{\sqrt{x^2 - L^2}} \tag{C15}$$

so the boat speed is

$$U_0 = -\frac{2}{\pi}\int_{-\infty}^{-L} \mathrm{Im}[f(z)]\frac{dx}{\sqrt{x^2 - L^2}} + \int_{L}^{\infty} \mathrm{Im}[f(z)]\frac{dx}{\sqrt{x^2 - L^2}}. \tag{C16}$$

Now (36) can be used:

$$\frac{U_0\pi}{2} = \frac{\beta}{4\mu}\left[\int_{-\infty}^{-L} \Gamma^- e^{\lambda(L+x)}\frac{dx}{\sqrt{x^2 - L^2}} + \int_{L}^{\infty} \Gamma^+ e^{\lambda(L-x)}\frac{dx}{\sqrt{x^2 - L^2}}\right]. \tag{C17}$$

On rearrangement this gives

$$U_0 = \frac{\beta(\Gamma^- - \Gamma^+)e^{\lambda L}}{2\pi\mu}\int_{L}^{\infty} e^{-\lambda x}\frac{dx}{\sqrt{x^2 - L^2}} = \frac{\beta(\Gamma^- - \Gamma^+)e^{\lambda L}}{2\pi\mu}\int_{1}^{\infty} e^{-\lambda L u}\frac{du}{\sqrt{u^2 - 1}}. \tag{C18}$$

Use of (13) and a result on an integral representation of the zeroth-order Bessel function already invoked in (B18) and (B19) of Appendix B leads to

$$U_0 = \frac{\Delta\sigma e^{\lambda L}}{2\pi\mu}K_0(\lambda L), \tag{C19}$$

which coincides with our earlier result (1).

[1] A. Zöttl and H. Stark, Emergent behavior in active colloids, J. Phys.: Condens. Matter **28**, 253001 (2016).

[2] N. J. Suematsu and S. Nakata, Evolution of self-propelled objects: From the viewpoint of nonlinear science, Chem. Eur. J. **24**, 6308 (2018).

[3] S. Nakata, M. Nagayama, H. Kitahata, N. J. Suematsu, and T. Hasegawa, Physicochemical design and analysis of self- propelled objects that are characteristically sensitive to environments, Phys. Chem. Chem. Phys. **17**, 10326 (2015).

[4] K. Dietrich, N. Jaensson, I. Buttinoni, G. Volpe, and L. Isa, Microscale Marangoni Surfers, Phys. Rev. Lett. **125**, 098001 (2020).

[5] A. Würger, Thermally driven Marangoni surfaces, J. Fluid Mech. **752**, 589 (2014).

[6] J. W. M. Bush and D. L. Hu, Walking on water: Biolocomotion at the interface, Ann. Rev. Fluid Mech. **38**, 339 (2006).

[7] E. Chevallier, A. Mamane, H. A. Stone, C. Tribet, F. Lequeuxa, and C. Monteux, Pumping-out photo-surfactants from an air–water interface using light, Soft Matter **7**, 7866 (2011).

[8] A. Diguet, R.-M. Guillermic, N. Magome, A. Saint-Jalmes, Y. Chen, K. Yoshikawa and D. Baigl, Photomanipulation of a droplet by the chromocapillary effect, Angew. Chem., Int. Ed. **48**, 9281 (2009).

[9] S. N. Varanakkottu, S. D. George, T. Baier, S. Hardt, M. Ewald, and M. Biesalski, Particle manipulation based on optically controlled free surface hydrodynamics, Angew. Chem., Int. Ed. **52**, 7291 (2013).

[10] H. Kitahata, S Hiromatsu, Y. Doi, S. Nakata, and M. R. Islam, Self-motion of a camphor disk coupled with convection, Phys. Chem. Chem. Phys. **6**, 2409 (2004).

[11] Y. S. Ikura, R. Tenno, H. Kitahata, N. J. Suematsu, and S. Nakata, Suppression and regeneration of camphor-driven Marangoni flow with the addition of sodium dodecyl sulfate, J. Phys. Chem. B **116**, 992 (2012).

[12] K. Ikeda, S.-I. Ei, M. Nagayama, M. Okamoto, and A. Tomoeda, Reduced model of a reaction-diffusion system for the collective motion of camphor boats, Phys. Rev. E **99**, 062208 (2019).
[13] H. Kitahata and N. Yoshinaga, Effective diffusion coefficient including the Marangoni effect, J. Chem. Phys. **148**, 134906 (2018).
[14] T. Bickel, Spreading dynamics of reactive surfactants driven by Marangoni convection, Soft Matter **15**, 3644 (2019).
[15] S. Jafari Kang, S. Sur, J. P. Rothstein, and H. Masoud, Forward, reverse, and no motion of Marangoni surfers under confinement, Phys. Rev. Fluids **5**, 084004 (2020).
[16] V. Vandadi, S. Jafari Kang, and H. Masoud, Reverse Marangoni surfing, J. Fluid Mech. **811**, 612 (2017).
[17] H. Masoud and H. A. Stone, A reciprocal theorem for Marangoni propulsion, J. Fluid Mech. **741**, R4 (2014).
[18] S. Soh, K. J. M. Bishop, and B. A. Gryzbowski, Dynamic self-assembly in ensembles of camphor boats, J. Phys. Chem. B **112**, 10848 (2008).
[19] N. J. Suematsu, S. Nakata, A. Awazu, and H. Nishimori, Collective behavior of inanimate boats, Phys. Rev. E, **81**, 056210 (2010)
[20] D. G. Crowdy, Collective viscous propulsion of a two-dimensional flotilla of Marangoni boats, Phys. Rev. Fluids **5**, 124004 (2020).
[21] E. Lauga and A. M. J. Davis, Viscous Marangoni propulsion, J. Fluid Mech. **705**, 120 (2012).
[22] H. Jin, A. Marmur, O. Ikkala, and R. H. A. Ras, Vapour-driven Marangoni propulsion: Continuous, prolonged and tunable motion, Chem. Sci. **3**, 2526 (2012).
[23] D. G. Crowdy, Surfactant-induced stagnant zones in the Jeong-Moffatt free surface Stokes flow problem, Phys. Fluids. **25**, 092104 (2013).
[24] M. Siegel, Influence of surfactant on rounded and pointed bubbles in two-dimensional Stokes flow, SIAM J. Appl. Math. **59**, 1998 (1999).
[25] D. Halpern and A. L. Frenkel, Destabilization of a creeping flow by interfacial surfactant: Linear theory extended to all wavenumbers, J. Fluid Mech. **485**, 191 (2003).
[26] G. Watson, *A Treatise on the Theory of Bessel Functions* (Cambridge University Press, Cambridge, 1995).
[27] D. G. Crowdy, Perturbation analysis of subphase gas and meniscus curvature effects for longitudinal flows over superhydrophobic surfaces, J. Fluid Mech. **822**, 307 (2017).
[28] T. Kirk, G. Karamanis, D. G. Crowdy, and M. Hodes, Thermocapillary stress and meniscus curvature effects on slip lengths in ridged microchannels, J. Fluid Mech. **894**, A15 (2020).
[29] D. G. Crowdy, Effect of shear thinning on superhydrophobic slip: Perturbative corrections to the effective slip length, Phys. Rev. Fluids **2**, 124201 (2017).
[30] E. Yariv and D. G. Crowdy, Phoretic self-propulsion of Janus disks in the fast-reaction limit, Phys. Rev. Fluids **5**, 112001(R) (2020).
[31] J.-T. Jeong and H. K. Moffatt, Free-surface cusps associated with flow at low Reynolds number, J. Fluid Mech. **241**, 1 (1992).
[32] D. G. Crowdy, *Solving Problems in Multiply Connected Domains*, NSF-CBMS Regional Conference Series in Applied Mathematics (Society for Industrial and Applied Mathematics, Philadelphia, 2020).
[33] D. J. Acheson, *Elementary Fluid Dynamics* (Oxford University Press, New York, 1990).
[34] M. Ablowitz and A. S. Fokas, *Complex Variables* (Cambridge University Press, Cambridge, UK, 1997).
[35] D. G. Crowdy, The Schwarz problem in multiply connected domains and the Schottky-Klein prime function, Complex Var. Elliptic Equations **53**, 221 (2008).